

## Growth and microstructure of synthetic chrysotile

KEIJI YADA

Research Institute for Scientific Measurements  
Tohoku University, Sendai, Japan

AND KAZUAKI IISHI

Department of Mineralogical Sciences and Geology  
Faculty of Literature and Science  
Yamaguchi University, Yamaguchi, Japan

### Abstract

Serpentine minerals were synthesized from  $2\text{Mg}_2\text{SiO}_4$  (natural olivine) +  $3\text{H}_2\text{O}$ , under various conditions for periods of 30 min to 30 days, to investigate the initial stages of chrysotile formation. Growth patterns and structures of the synthetic chrysotile were examined by means of X-ray, electron diffraction, and lattice-imaging electron microscopy. It is suggested that chrysotile cylinders grow at both the tips and roots of fibers by addition at the growth front. This mechanism basically supports the model of Jagodzinski and Kunze (1954).

Microstructures of synthetic chrysotile observed by lattice imaging are described, and the fine structure in electron diffraction patterns of chrysotile is qualitatively explained by a differential refraction effect.

### Introduction

Chrysotile, lizardite, and antigorite are typical varieties of serpentine minerals with different morphologies. Why and how such varieties are formed is not fully understood. One of the authors (Yada, 1967, 1971) found that the lattice-imaging method of high-resolution electron microscopy is very effective for observing the microstructure of chrysotile, and for understanding its growth mechanism. In order to elucidate the growth mechanism in more detail, it seems necessary to study the microstructure of serpentine minerals synthesized in a controlled manner. Consequently, we studied the influence of pH, reaction temperature, and reaction time on the morphological and structural features of synthetic chrysotile (Yada and Iishi, 1974). We found that the initial nuclei of chrysotile in neutral solutions are membranous sheets consisting of a few unit layers, formed within 30 min at  $300^\circ$  to  $400^\circ\text{C}$ , and then curled up into conical or cylindrical fibrils.

In this paper, the initial stages of growth under alkaline and acidic conditions and the growth mechanism of chrysotile will be discussed on the bases of microstructures observed for the synthetic material. Finally, fine detail of the electron diffraction patterns will be interpreted in terms of an electron refraction

effect caused by the circular cross-section of the chrysotile fibrils.

### Experimental methods

Several possible ways of serpentinization in nature, starting from different matrices such as olivine, pyroxene or/and silica, have been proposed (Deer *et al.*, 1962, p. 185-187). On the other hand, hydrothermal synthesis of serpentine minerals has been reported by many workers from various kinds of starting minerals. In our experiments, natural olivine<sup>1</sup>

<sup>1</sup> Composition by chemical analysis (standard conventional silicate analytical method) is as follows (Aoki and Shiba, 1974)

SiO <sub>2</sub>	40.70
TiO <sub>2</sub>	0.01
Al <sub>2</sub> O <sub>3</sub>	0.20
Fe <sub>2</sub> O <sub>3</sub>	none
FeO	9.77
MnO	0.13
MgO	48.77
NiO	0.38
CaO	0.07
Na <sub>2</sub> O	none
K <sub>2</sub> O	none
H <sub>2</sub> O±	none
total	100.03

from Itinome-gata Akita Prefecture, Japan, pulverized to have the grain size of  $0.1\mu \sim 2\mu$ , was selected as a starting material for the synthesis.

The experimental apparatus and the procedure for the chrysotile synthesis are the same as those already reported (Yada and Iishi, 1974). Synthesis was carried out under neutral conditions, and in highly alkaline (1N NaOH) or acidic (0.3N HCl) solutions. The products, quenched to room temperature, were rinsed with distilled water and examined by means of X-ray, electron diffraction, lattice-imaging electron microscopy, and optical diffraction of electron micrographs.

### Results and discussion

The experimental conditions and results are listed in Table 1. The pH values refer to those of the starting solution. The pH of the solution quenched after reaction was not measured. The reaction temperatures,  $300^\circ$  and  $400^\circ\text{C}$ , were selected as the most suitable for chrysotile formation (Yada and Iishi, 1974). The essential reaction is thought to be:  $2\text{Mg}_2\text{SiO}_4 + 3\text{H}_2\text{O} = \text{Mg}_3\text{Si}_2\text{O}_5(\text{OH})_4 + \text{Mg}(\text{OH})_2$ . Initial nuclei of serpentine were observable with an electron microscope after 30 min hydrothermal treatment, although no traces of serpentine were detected by X-ray diffraction. After several days, serpentine and brucite were always recognized by X-ray analysis. Magnetite, which might be formed in this experiment, was not detected, though recent work by Moody (1976) showed that the serpentinization of Fe-bearing olivine produces magnetite in addition to serpentine and brucite.

Table 1. Synthesis conditions and results

Run no.	pH	T(°C)	Time	Varieties	Shape of C	Type of C
OS 121	7	300	30 m	O>>C		
OS 123	7	300	2 hr	O>>C		
OS 111	7	300	5 hr	O>>C		
OS 112	7	300	30 d	C	conical>>parallel	clino<para
OS 122	7	400	30 m	O>>C		
OS 124	7	400	2 hr	O>>C		
OS 114	7	400	5 hr	O>>C,L	conical>parallel	
OS 115	7	400	30 d	C,L	conical>parallel	clino<para
OS 141	13.6*	300	30 m	O>>C		
OS 142	13.6*	300	5 hr	O=C	conical<parallel	clino=para
OS 002'	13.6*	300	10 d	C	conical<parallel	clino>para
OS 003'	13.6*	400	10 d	C	conical<parallel	clino>para
OS 143	0.8**	300	30 m	O>>C		
OS 144	0.8**	300	5 hr	O>>C,L	conical>>parallel	clino=para
OS 131	0.8**	300	10 d	O,C	conical>>parallel	clino<para
OS 132	0.8**	400	10 d	C	conical=parallel	clino<para

\*1N NaOH, \*\*0.3N HCl

Pressure 700 bar, C:chrysotile, L:lizardite, O:olivine. Relative amounts of the serpentine varieties and classification of chrysotile fibrils were roughly estimated by electron microscopy and electron diffraction.

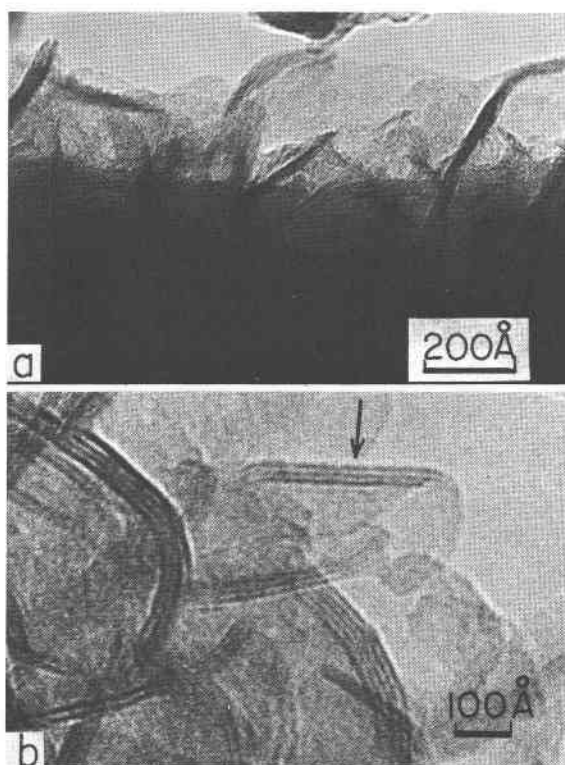


Fig. 1 Membranous nuclei formed on the surface of olivine (a) after 30 min treatment at  $300^\circ\text{C}$ , pH 7 (Run OS 121), (b) after 2 hr treatment at  $300^\circ\text{C}$ , pH 7 (Run OS 123).

#### (1) Growth under neutral conditions

Figure 1 shows the initial stages of serpentinization at  $300^\circ\text{C}$  for 30 min (a) and 2 hr (b). Slightly curved membranes having a rather rough surface on a molecular level, and consisting of a few unit layers several hundred Angstrom units wide are seen on the surface of the olivine. These initial membranes seem to be curved in various ways so as to form parts of a sphere, cone, or cylinder, depending on the ambient conditions, especially on pH and temperature. With longer treatment they formed conical or cylindrical fibrils by further wrapping of the curved membranes as shown in Figure 1b. The nucleus, indicated by the arrow, is conical with a wall only three layers thick; its appearance is characteristic of parachrysotile, as shown by the direction of the 4.5Å fringes parallel to the arrow. The membranes contain an even or odd number of unit layers. The smallest number of observable layers is one.

Figure 2 shows another example from the sample prepared at  $300^\circ\text{C}$  for 2 hr, with the corresponding diffraction patterns. Many nuclei are seen around the olivine particle (a); (b) is an enlarged image of a part

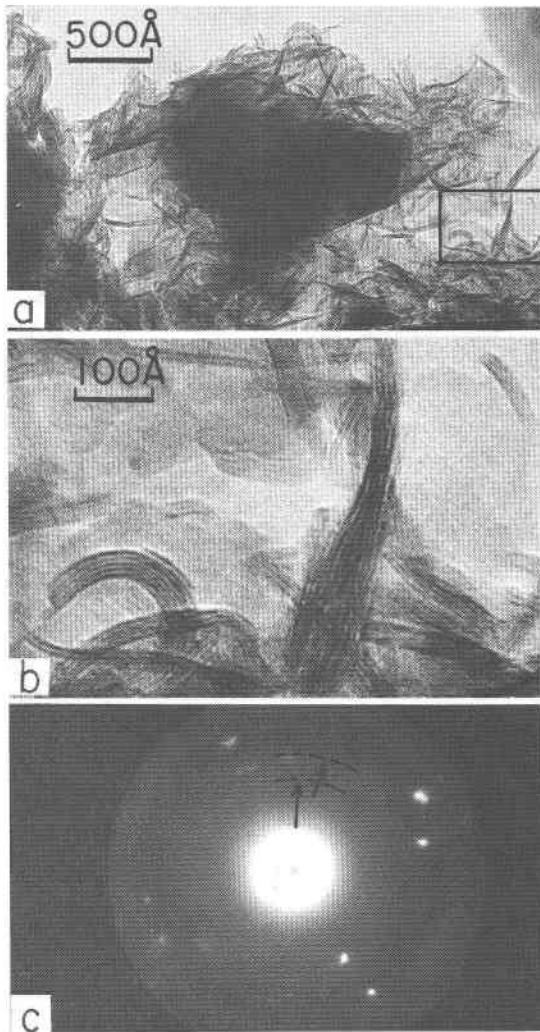


Fig. 2 Membranous nuclei formed after 2 hr treatment at 300°C, pH 7 (Run OS 123) (a) low-magnification image, (b) enlarged image, (c) electron diffraction pattern.

of (a), and (c) the electron diffraction pattern. The intense diffraction spots in (c) are from olivine, and the arrows indicate the position of the diffraction rings of chrysotile corresponding to 7.3 Å and 4.5 Å spacings. These very faint and diffuse rings suggest that the crystallinity of the initial nuclei is still poor at this stage.

Figure 3 shows, at low and high magnifications, the stage of serpentinization by hydrothermal treatment at 400°C for 2 hr. Many serpentine membranes consisting of several unit layers have grown in a relatively flat shape from the surface of the olivine particle. Most of these flat membranes curl up with increased hydrothermal treatment time. Some of them remain

flat, and eventually become lizardite, identifiable by selected-area electron diffraction. These platy crystallites often showed well-defined hexagonal form and mosaic domain structure of 4.5 Å lattice fringes including many dislocations (Yada and Ishi, 1974), but neither the long-period lattice fringes nor the superlattice diffraction pattern characteristic of antigorite.

Figure 4a shows a typical cone-in-cone morphology (Bates and Comer, 1957), obtained after 30 days treatment at 300°C, while Figure 4b shows that platy lizardite is formed concurrently with normal straight and conical fibrils of chrysotile at the higher temperature, 400°C.

### (2) Growth under alkaline conditions

Serpentinization is much faster in a highly alkaline solution of 1N NaOH, and cylindrical chrysotile fibrils of several hundred Angstrom units in length are formed within 30 min, as shown in Figure 5a. Some of these fibrils have very thin walls at this stage, but they grow rather rapidly and several hours later become straight with a diameter and wall thickness

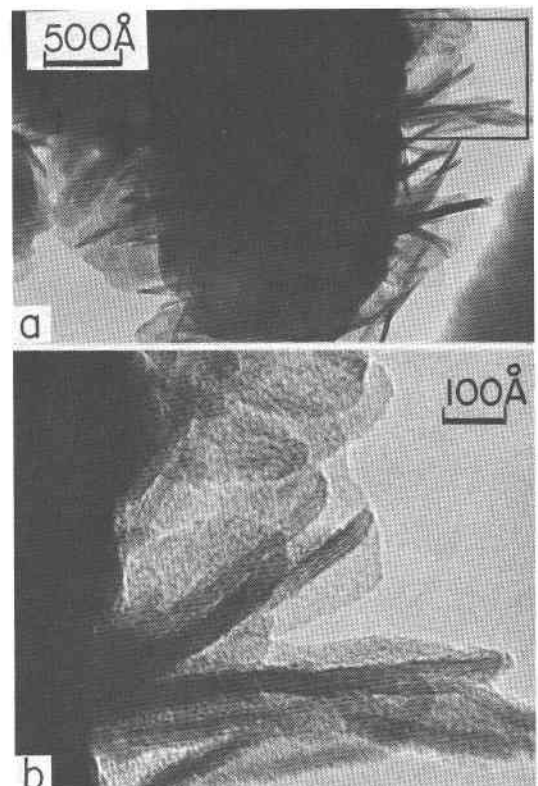


Fig. 3 Initial stage of serpentinization after 2 hr treatment at 400°C, pH 7 (Run OS 124).

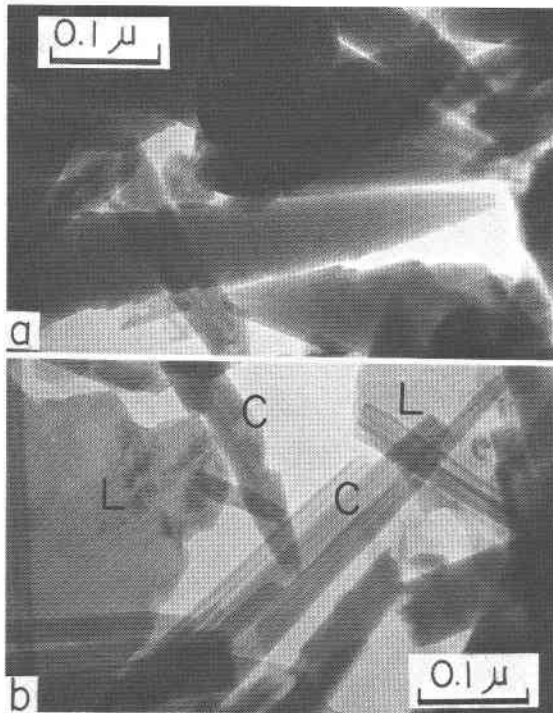


Fig. 4 (a) Cone-in-cone fibrils of chrysotile after 30 days at 300°C, pH 7 (Run 112), (b) chrysotile (C) and lizardite (L) after 30 days at 400°C, pH 7 (Run OS 115).

similar to those of natural chrysotile. Figure 5b shows such an example obtained by a 5 hr treatment, where many straight or slightly conical fibrils have grown radially from the surface of olivine particle like spines of a sea-urchin. These fibrils also show various growth patterns if observed by optical diffraction (Yada and Iishi, 1974).

### (3) Growth under acidic conditions

In a highly acidic solution, rather wide and slightly curved membranes consisting of several unit layers were formed on the olivine and then gradually wrapped up to form chrysotile fibrils. Figure 6 shows a typical example from a 30 min hydrothermal treatment at 300°C. Portion *A* is a side view of a membrane growing from the surface of the olivine, about 10 unit layers thick. The spacing of the unit layers is not uniform throughout, especially at their root, *B*. At *C*, very small initial nuclei, 1–2 unit layers thick, have grown in an oriented direction, which suggests a preferential growth relation between the olivine and serpentine layers.

Figure 7a shows at a relatively low magnification an example of a 5 hr treatment at 300°C. Most of

the membranes are beginning to wrap into a conical shape. Figure 7b shows the conical fibrils obtained after 10 days hydrothermal treatment at 300°C. Cone-in-cone fibrils grow in such a manner that the bases of the conical fibrils are in contact with the olivine (left top of the picture) and the tip is always tapered.

From these observations of the initial stages of serpentinization, the growth mechanism of chrysotile from olivine may be described phenomenologically as shown in Figure 8. The initial nuclei of serpentine are formed after 20–30 min reaction as membranes of several unit layers thick and a few hundred Angstrom units wide, protruding from the surface of olivine. There will be various kinds of ions such as  $(\text{Si}_2\text{O}_5)^{2-}$ ,  $\text{Mg}^{2+}$ , and  $(\text{OH})^-$  in the hydrothermal solution, and initial nucleation of serpentine will take place at the sites where these component ions coalesce, either apart from or attaching to the olivine in the solution, under a certain supersaturation condition. The experimental results showed that the latter case is much more frequent. Crystallinity at this stage is rather poor. Nuclei are curved as a part of a sphere, cone,

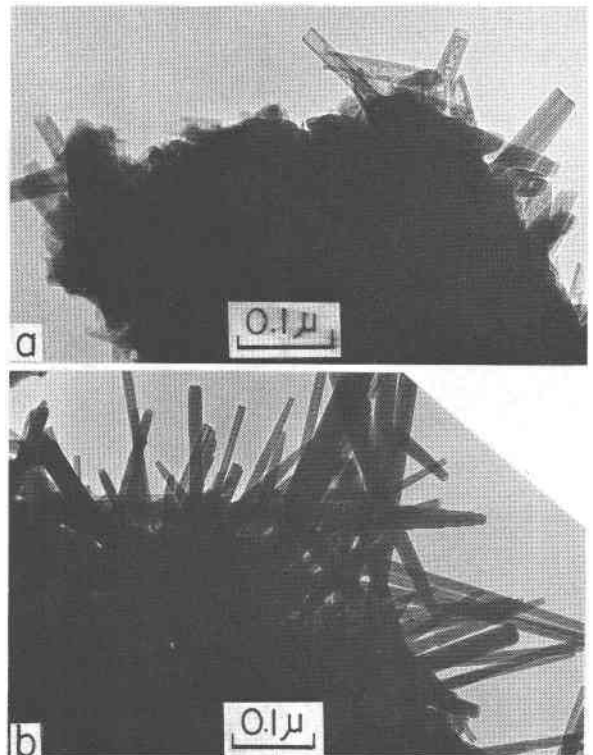


Fig. 5 Initial stages of serpentinization at 300°C under alkaline conditions (a) 30 min treatment (Run OS 141), (b) 2 hr treatment (Run OS 142).

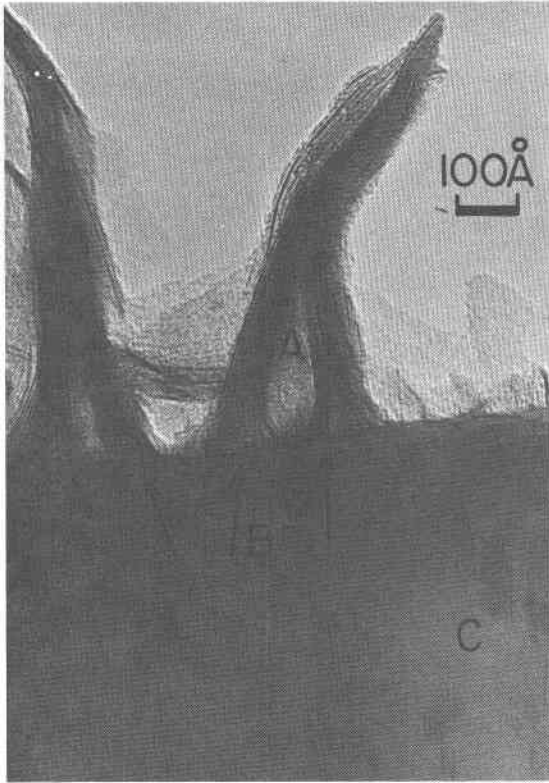


Fig. 6 Initial stage of serpentinization after 30 min treatment at 300°C under acidic conditions (Run OS 143).

or cylinder, depending on the ambient conditions of pH, temperature, and additives, and the membranes grow and wrap up to form conical or cylindrical fibrils. In alkaline solutions, cylindrical wrapping is likely to occur from the beginning of the growth of the membrane, but in acidic solution the membrane first spreads to some extent and then the curling starts. In stage (b), a perfectly round connection which leads to a concentric crystal may be possible, especially in alkaline solutions, but the spiral folding is much more general, and leads to the conical or cylindrical structure with a spiral arrangement.

With respect to the mechanism of the growth of the serpentine layers, molecular particles or clusters with serpentine compositions formed by coalescence of the component ions from decomposition of the olivine in the hot solution will reach the membrane, and diffuse on the outer or inner surface of the wrapped membrane and settle at kink sites in the layer front.<sup>2</sup> Thus

<sup>2</sup> It is still not clear whether the component ions form "molecular particles or clusters" by diffusion before they settle to the kink sites, or directly assemble at the kink sites so as to crystallize into the serpentine layer, but the former case seems plausible.

the fibrils become longer (a kind of tip growth) and thicker by advancement of the layer front as shown in Figures 8c and 8d, where the growth mechanism of Jagodzinski and Kunze (1954) may operate.

In the vicinity of the interface between the olivine and the membrane, the component ions for serpentinization are supplied more easily to kink sites near the root of membranes from the olivine matrix. Thus, root growth advancing toward the decomposing matrix, as well as tip growth, will take place. Actually, there will be a high density of nuclei, so that the growth form is like spines of a sea-urchin. Growth will cease when decomposition of the olivine particle is finished (Fig. 8d).

In the growth of natural chrysotile, in places where hydrothermal water penetrates into narrow cracks of the matrix rock, many nuclei are formed at the same time, so that the axial directions of the fibrils will be lined perpendicularly to the rock face. The bundles of fibrils will then grow towards the decomposing rock face, leaving a gap between the two sides. Such a plane of discontinuity, which represents the contact

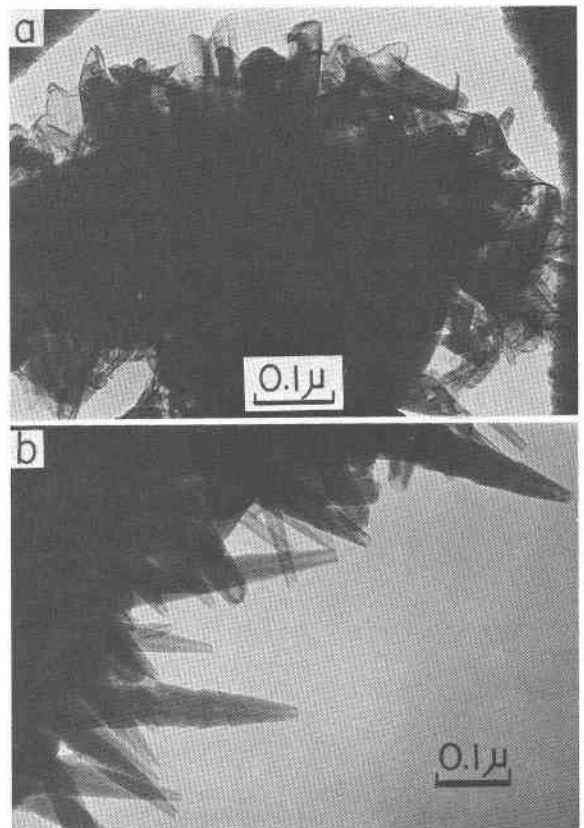


Fig. 7 Initial stage of serpentinization under acidic conditions (a) after 2 hr treatment at 300°C (Run OS 144), (b) after 10 days at 300°C (Run OS 131).

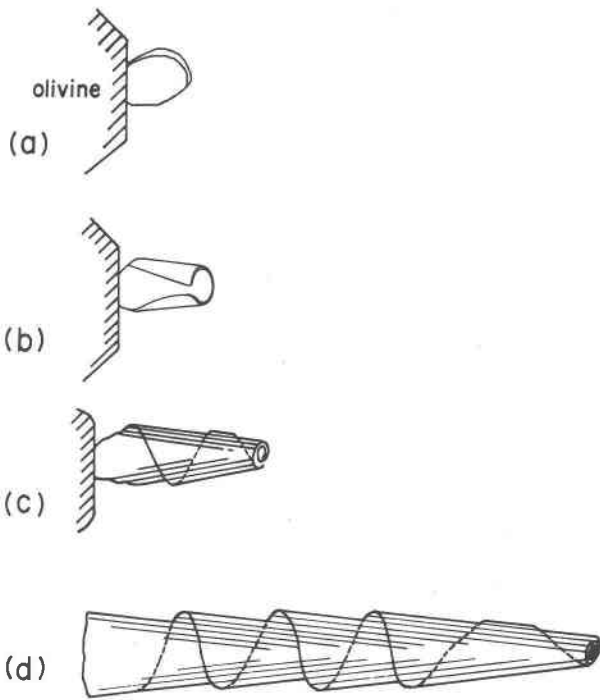


Fig. 8 Schematic drawing of chrysotile formation.

area of the growth fronts from the two sides, is usually observed near the middle of a vein of a so-called cross-fiber deposit.

The control of oxygen partial pressure ( $f_o$ ) is very important from a petrological point of view in an iron-bearing system, but we did not attempt it. Our preliminary experiment with a synthetic iron-free olivine showed that the growth mechanism of chrysotile was not affected much by iron content. The results obtained with the synthetic olivine and olivine formed from natural chrysotile will be reported elsewhere.

#### (4) Microstructure of synthetic chrysotile

As already reported (Yada and Iishi, 1974), parachrysotile rather than ortho- or clinochrysotile is frequently identified in the synthetic sample. Figure 9 shows a typical example of parachrysotile with a small conical formed under acidic conditions (0.3N HCl, 400°C, 10 days). It is identified by the 4.5Å fringes intersecting the 7.3Å fringes at right angles. The 4.5Å fringes are not always visible over all areas, but are confined to certain lattice planes. This seems to be caused by the failure of regular crystallographic stacking in the  $a$ - $b$  plane between adjoining membranes, resulting from the wrapping and advancement of the initial membranes as they grow into the conical shape. As regular stacking can hold for a

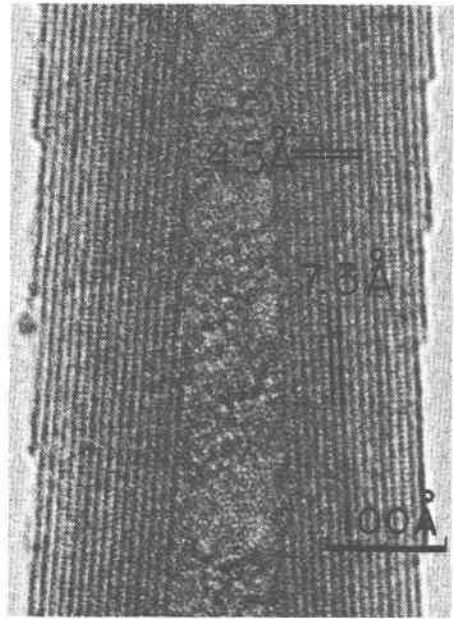


Fig. 9 A typical example of parachrysotile with a weak conical component (Run OS 132).

helical roll but not for a conical roll, it is reasonable to suppose that the intermembrane binding is very weak, and therefore voids or cavities are sometimes observed between the adjoining membranes of conical fibrils, even when they are not heavily damaged by the electron beam during observation.

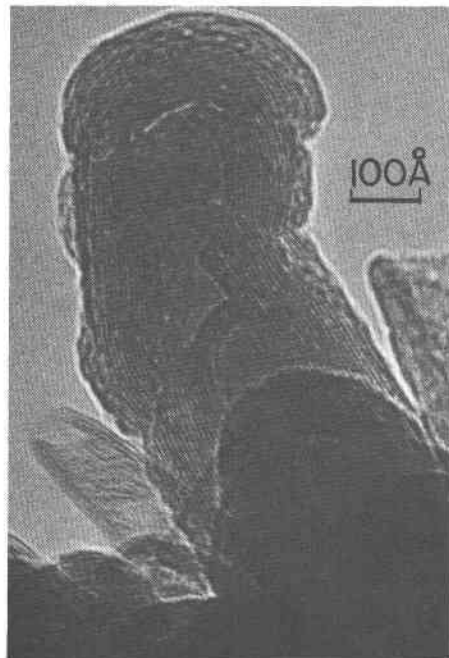


Fig. 10 Microstructure of a fibril showing bump-like growth (Run OS 144).



Morphologically-complicated chrysotile crystals are sometimes formed during growth from the initial membranous nuclei to the wrapped fibrils, as a result of mutual contact between nuclei producing deformation or superposition. Figure 10 shows a bump-like growth, suggesting a spherical curvature of the crystal plane at the tip.

The other morphological type is a Y-shaped intergrowth as already reported by Bates and Comer (1957) in a synthetic sample. Figure 11 shows an example of a Y-shaped intergrowth observed in the case of acidic solution. The two Y-shaped fibrils (*A* and *B*) have connection angles of about 38° and 60° respectively. The interconnection behavior of the lattice fringes of fibril *A* seems to suggest some crystallographic relation such as twinning between the two branches. Structurally, the longer arm of *A* is parachrysotile and the shorter arm is clinochrysotile, while those of *B* are both conical parachrysotile. These unusual types of growth are often encountered in synthetic chrysotile, especially for acidic growth

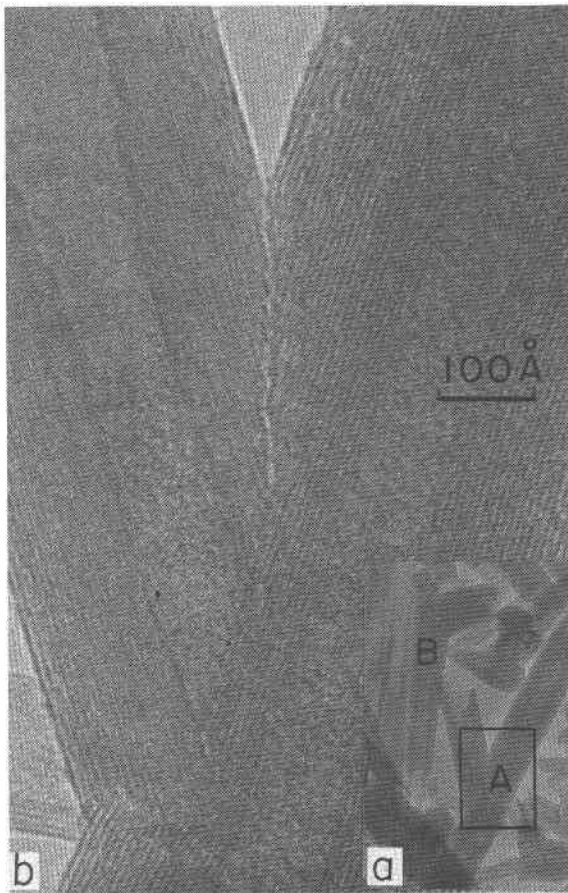


Fig. 11 Microstructure of Y-shaped intergrowth (Run OS 131).

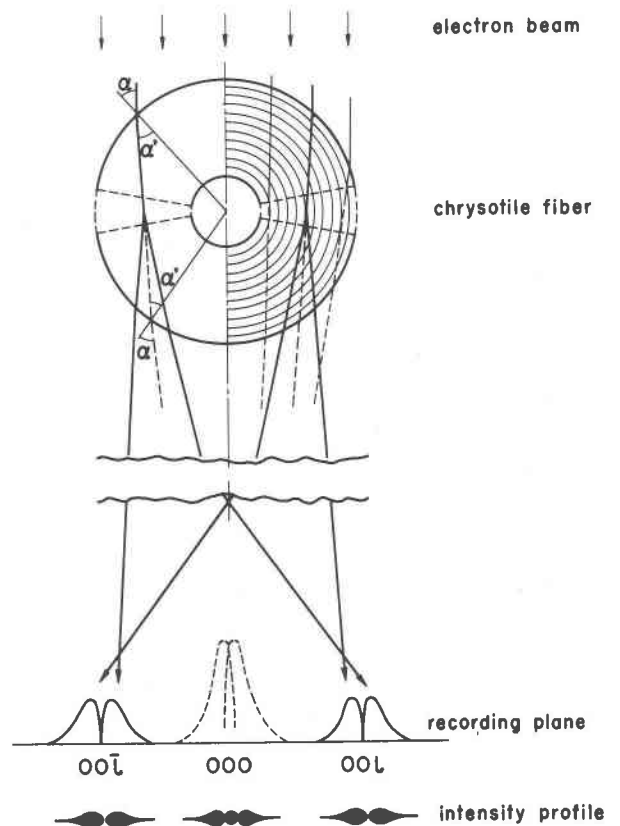


Fig. 12 Schematic drawing for the explanation of the splitting of the diffraction spots by refraction of the electron beam.

conditions, in contrast to the case of natural chrysotile.

It was reported by one of us (Yada, 1967) that the electron diffraction pattern taken with a divergent electron beam from a single fibril of natural chrysotile shows some fine structure, such as a splitting of the spots of the  $\{00l\}$  reflections. This phenomenon is observed not only for all kinds of chrysotile, but also for the other cylindrical minerals such as halloysite, and is interpreted qualitatively as a differential refraction of beams incident on and emerging from opposite surfaces of a cylinder, as shown in Figure 12. For refraction of an electron beam, the following equations hold,

$$\sin \alpha / \sin \alpha' = n \quad (1)$$

$$n = 1 + V_0/2E \quad (2),$$

where  $\alpha$  is the angle of incidence,  $\alpha'$  the angle of refraction,  $n$  the electron-optical refractive index,  $E$  the accelerating potential, and  $V_0$  the mean inner potential of the object. It has been reported that the mean inner potential  $V_0$  of chrysotile is about 11.6

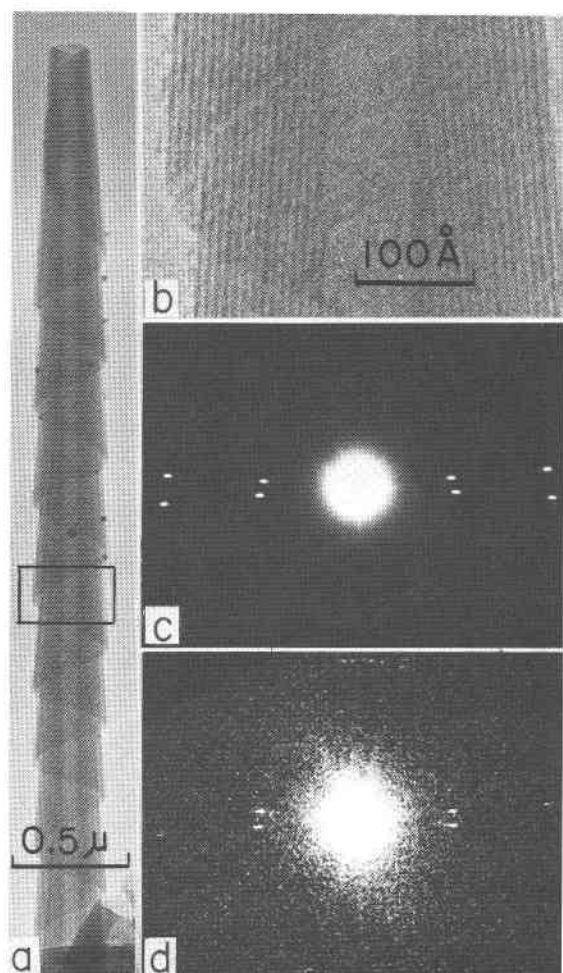


Fig. 13 An example of a cone-in-cone fibril showing split spots (Run OS 132) (a) low-magnification image, (b) enlarged image, (c) electron diffraction pattern, (d) optical diffraction pattern of (b).

volt (Yada *et al.*, 1973). For  $E = 100 \text{ kV}$  and  $V_0 = 11.6 \text{ V}$ ,  $n$  is 1.00006, which is very close to unity. Therefore the refraction effect is very small in general, but becomes appreciable at glancing incidence, when  $\alpha$  is close to  $90^\circ$ .

It seems reasonable to assume the following (a) the electron beam is refracted at both surfaces of the chrysotile; (b) according to equations (1) and (2), the refraction is greater towards the edge; (c) Bragg reflection takes place symmetrically inside the narrow sectors bounded by the dotted lines in Figure 12; (d) the intensity of the diffracted beam is stronger towards the edge because the outer layers are less curved, and the effective thickness for diffraction is greater. We can thus expect to have an intensity distribution with long tails for the split spots, as

schematically shown in Figure 12.<sup>3</sup> Usually, the splitting of the central spot is obscured by halation.

It can be seen that for a cone-in-cone the splitting takes place not on a straight line but on two intersecting lines depending on the cone angle, so that the split spots are not equidistant from the central spot. Figure 13 shows an example of a single chrysotile fiber formed in an acidic condition; (a) and (b) show images at low and high magnifications; (c) is the corresponding electron diffraction pattern and (d) the optical diffraction pattern from the electron micrograph. The electron diffraction spots corresponding to the 7.3 Å spacing of (002) and its higher order split into two non-equidistant spots (about 5% different), but the optical diffraction spots are nearly equidistant, which suggests that the actual spacing of the lattice fringes is the same on both sides. The electron and optical diffraction patterns also suggest that this fibril is parachrysotile.

<sup>3</sup> The dynamical double-refraction effect of an electron beam which is often observed for crystallites with a definite crystal habit, such as MgO, is neglected here.

### Acknowledgement

The authors thank Professor K. Aoki, Tohoku University, for supplying natural olivine and its chemical analysis.

### References

- Aoki, K. and I. Shiba (1974) Olivines from Iherzolite inclusions of Itinome-gata, Japan. *Mem. Geol. Soc. Japan*, 11, 1-10.
- Bates, T. F. and J. J. Comer (1957) Further observations on the morphology of chrysotile and halloysite. *Clays and Clay Minerals, Proc. 6th National Clay Conf.*, 237-248.
- Deer, W. A., R. A. Howie and J. Zussman (1962) *Rockforming Minerals*, Vol. 3, *Sheet Silicates*. Longmans, London.
- Jagodzinski, H. and G. Kunze (1954) Die Röllchenstruktur des Chrysotils III. Versetzungswachstum der Röllchen. *Neues Jahrb. Mineral. Monatsh.*, 137-150.
- Moody, J. B. (1976) An experimental study on the serpentinization of iron-bearing olivines. *Can. Mineral.*, 14, 462-478.
- Yada, K. (1967) Study of chrysotile asbestos by a high resolution electron microscope. *Acta Crystallogr.*, 23, 704-707.
- (1971) Study of microstructure of chrysotile asbestos by high resolution electron microscope. *Acta Crystallogr.*, A27, 659-664.
- , K. Shibata and T. Hibi (1973) A high resolution electron interference microscope and its application to the measurement of mean inner potential. *J. Electronmicroscopy*, 22, 223-230.
- , and K. Iishi (1974) Serpentine minerals hydrothermally synthesized and their microstructures. *Crystal Growth*, 24/25, 627-630.